Drug Development and Industrial Pharmacy

http://informahealthcare.com/ddi
ISSN: 0363-9045 (print), 1520-5762 (electronic)

Drug Dev Ind Pharm, Early Online: 1–10
 DOI: 10.3109/03639045.2013.790408

informa healthcare

ORIGINAL ARTICLE

Characterization, inclusion mode, phase-solubility and *in vitro* release studies of inclusion binary complexes with cyclodextrins and meglumine using sulfamerazine as model drug

Carolina Aloisio[1,2], Anselmo Gomes de Oliveira[2], and Marcela Longhi[1]

[1]Departamento de Farmacia, Facultad de Ciencias Químicas, UNITEFA (CONICET), Universidad Nacional de Córdoba, Ciudad Universitaria, X5000HUA Córdoba, Argentina and [2]Departamento de Farmácia, Faculdade de Ciências Farmacêuticas, Universidade Estadual Paulista, Rodovia Araraquara-Jau km 1, 14800-900 Araraquara – SP, Brazil

Abstract

In order to investigate the effect on the aqueous solubility and release rate of sulfamerazine (SMR) as model drug, inclusion complexes with β-cyclodextrin (βCD), methyl-β-cyclodextrin (MβCD) and hydroxypropyl-β-cyclodextrin (HPβCD) and a binary system with meglumine (MEG) were developed. The formation of 1:1 inclusion complexes of SMR with the CDs and a SMR:MEG binary system in solution and in solid state was revealed by phase solubility studies (PSS), nuclear magnetic resonance (NMR), Fourier-transform infrared spectroscopy (FT-IR), thermal analysis and X-Ray diffractometry (XRD) studies. The CDs solubilization of SMR could be improved by ionization of the drug molecule through pH adjustments. The higher apparent stability constants of SMR:CDs complexes were obtained in pH 2.00, demonstrating that CDs present more affinity for the unionized drug. The best approach for SMR solubility enhancement results from the combination of MEG and pH adjustment, with a 34-fold increment and a S_{max} of 54.8 mg/ml. The permeability of the drug was reduced due to the presence of βCD, MβCD, HPβCD and MEG when used as solubilizers. The study then suggests interesting applications of CD or MEG complexes for modulating the release rate of SMR through semipermeable membranes.

Keywords

Complexation, cyclodextrin, meglumine, permeability, sulfamerazine

History

Received 3 July 2012
Revised 25 March 2013
Accepted 25 March 2013
Published online 29 April 2013

Introduction

The sulfonamides are synthetic bacteriostatic antimicrobials with a wide spectrum against most Gram-positive and many Gram-negative organisms. Nowadays, the main use of sulfonamides is for the treatment of urinary tract infections. Other uses of these drugs include systemic infections and ophthalmic preparations. Sulfamerazine (SMR) (Figure 1a) is a very slightly water-soluble drug according to European Pharmacopoeia[1], and although it is not yet classified in the Biopharmaceutics Classification System, sulfadiazine, which is a structural analogue, was classified as IV, due to its low permeability and solubility[2]. Because SMR is slowly excreted by the kidneys, while offering higher blood levels, the kidneys have an increased chance of crystalluria[3]. Additionally, the absorption of SMR from the gastrointestinal tract does not lead to values high enough to avoid the need for parenteral administration of the drug when high levels are required. Concerning the drawbacks associated with the SMR treatment, the use of suitable strategies to increase its water solubility or gastrointestinal absorption could reduce the undesirable side effects by the administration of lower doses. Also, experimental approaches applied on this drug could be extrapolated to other poor water-soluble active ingredients. It is well described that the use of some drug carriers can increase the solubility and modulates the transport and/or the release of drugs to specific sites[4–9].

β-Cyclodextrin (βCD) is a truncated-cone polysaccharide composed of seven α-D-glucopyranoside monomers linked by 1,4-glucose bonds. Cyclodextrins can encapsulate model substrates to form host–guest complexes or supramolecular species in aqueous solutions and in solid states, fact that it is successfully utilized for the improvement of pharmaceutical properties of drugs[10,11]. Various cyclodextrin derivatives have been developed during the past decades[12–18], which extensively expanded the applications of these cyclic oligosaccharides and overcome the serious issues of parent CDs such as low water solubility and toxicity. For instance, substitution of the hydroxyl groups may disrupt the hydrogen bonds and significantly increase their aqueous solubility. Complexation of these βCD derivatives, such as the methylated βCD (MβCD) and hydroxypropylated βCD (HPβCD) ones (Figure 1b)[19], with active molecules exhibit different properties from their original free forms and usually result in enhancement of aqueous solubility[20,21], better chemical stability[22,23], and increased permeability and bioavailability of drugs[24,25]. The total solubility of a drug in the presence of CDs can be highly enhanced by pH adjustment or the use of a proper third component[26–28].

Address for correspondence: Marcela Longhi, Departamento de Farmacia, Facultad de Ciencias Químicas, UNITEFA (CONICET), Universidad Nacional de Córdoba. Ciudad Universitaria, X5000HUA Córdoba, Argentina. E-mail: mrlcor@fcq.unc.edu.ar

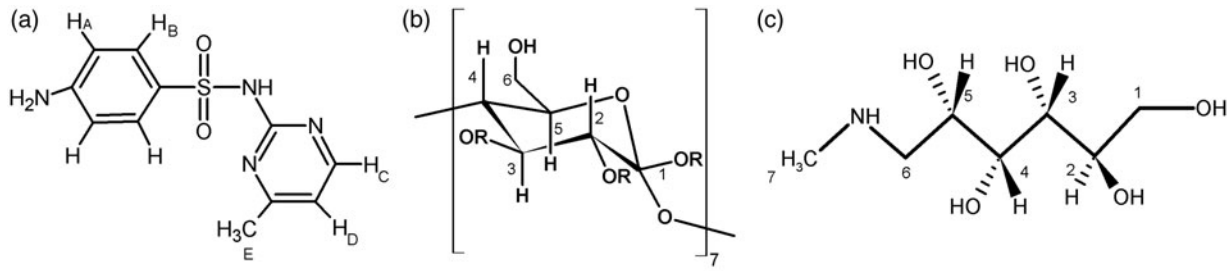

Figure 1. Chemical structure of: (a) SMR; (b) βCD, MβCD or HPβCD when R = H; $-CH_3$ or $-CH_2CH(OH)CH_3$, respectively; (c) MEG.

Also, many other strategies to revert unacceptable properties of active molecules have been reported[4,29,30]. Salt formation is a well-established and effective technique for increasing solubility and dissolution rates and consequently the oral bioavailability of acidic and basic drugs[31,32], and hence is very important for the selection of a suitable counterion. N-acetyl glutamine, also known as meglumine (MEG), is a polyhydroxy organic amine (Figure 1c) that demonstrated to raise solubility[33], drug release rate[34,35] and stabilization[36] of weakly acidic molecules.

A recent study conducted in our laboratory has demonstrated the formation of a SMR:βCD inclusion complex with a fourfold enhancement on the drug solubility, reporting a stability constant value of 215 M^{-1} and attaining a water solubility of 0.8 mg/ml[37], using nuclear magnetic resonance (NMR), phase solubility analysis and molecular modeling. On this basis, the investigations were conducted not only to complement the previous study about the SMR:βCD complex by Fourier-transform infrared spectroscopy (FT-IR), thermal analysis [differential scanning calorimetry (DSC) and thermogravimetric analysis (TGA)] and X-ray diffractometry (XRD), but also for evaluating the formation of binary systems with other complexing agents such as MβCD, HPβCD and MEG. In addition, the effect of MEG and the CDs on SMR drug release from the complexes stoichiometric solutions was determined.

Methods

Materials

Sulfamerazine was obtained from Parafarm®, Argentina. Meglumine was purchased from Sigma Aldrich®, St. Louis, MO; βCD ($M_W = 1135$), MβCD ($M_W = 1190$) and HPβCD ($M_W = 1325$) were kindly supplied by Ferromet® (agent in Argentina of Roquette®). All the other materials and solvents were of analytical reagent grade. A Millipore Milli-Q Water Purification System generated the water used in these studies.

Phase solubility studies (PSS)

Solubility diagrams were obtained according to Higuchi and Connors method[38]. Each experiment was performed in triplicate. Excess amounts of SMR, for saturation conditions, were added to aqueous or buffered solutions containing βCD (0–16 mM), MβCD (0–100 mM), HPβCD (0–18 mM) or MEG (0–250 mM), in relation with their aqueous solubilities. The suspensions formed were sonicated in an ultrasonic bath for 15 min every 12 h to favor solubilization and then placed in a 25.0 ± 0.1 °C constant temperature bath [HAAKE DC10 thermostat (Haake®, Paramus, NJ)] for 72 h. After equilibrium was reached, the suspensions were filtered through a 0.45-μm membrane filter (Millipore®, Billerica, MA) and analyzed in a Shimadzu® UV-160 spectrophotometer. The equilibrium pH of each solution was measured (Hanna® HI 255 pH meter). The apparent stability constants (K_c) of the SMR:CD complexes were determined as a function of the added ligand concentration (CD)[21]. Because the phase solubility diagrams were of A_L-type and assuming a 1:1 complex, the apparent stability (or formation) constants K_c were calculated using the slope from the linear regression analysis of the phase solubility isotherms using the following equation:

$$K_c = \text{slope}/S_0(1 - \text{slope})$$

where S_0 is the solubility of the pure drug.

Nuclear magnetic resonance (NMR) studies

^{1}H NMR and 2D ROESY were performed at 298 K in a Bruker® Avance II High Resolution Spectrometer equipped with a Broad Band Inverse probe (BBI) and a Variable Temperature Unit (VTU) using 5 mm sample tubes. Espectra were obtained at 400.16 MHz. Based on the 1:1 stoichiometry data obtained in the PSS, equimolar ratio complexes and pure substances solutions were prepared in D_2O by incorporating an excess amount of the drug with a fixed concentration of each ligand that was sonicated for an hour to favor the maximum SMR solubilization to obtain a measurable concentration of the drug and to form the complexes. The suspensions were filtered before their analysis. The NMR data were processed with the Bruker TOPSPIN 2.0 software. The residual solvent signal (4.80 ppm) was used as the internal reference. Induced changes in the ^{1}H NMR chemical shifts (Δδ) for SMR originated due to their interaction with the ligands were calculated according to the following equation:

$$\Delta\delta = \delta_{\text{complex}} - \delta_{\text{free}}$$

Solid samples preparation

Freeze-dried systems (FDS) were obtained by the freeze-drying technique using a Labconco® Freeze Dye 4.5 equipment, at 40 ± 1 °C with 50 mbar vacuum for 24 h. Based on the 1:1 stoichiometry data obtained in the PSS, equimolar ratio complexes or binary systems and pure substances aqueous solutions were prepared by incorporating an excess amount of the drug with a fixed concentration of each ligand that was sonicated for an hour. The suspensions were filtered and then frozen at −40 °C until their complete solidification for the freeze-drying procedure. On the other hand, physical mixtures (PM) of the components were prepared using the same molar ratios, by simple mixing in agate mortar.

Fourier-transform infrared spectroscopy (FT-IR)

The FT-IR spectra of pure substances, FDS and PM were recorded as potassium bromide discs using a Nicolet 5 SXC FT-IR spectrometer. The signal changes of the corresponding functional groups were compared to analyze the mode of interaction between them.

Differential scanning calorimetry (DSC) and thermogravimetric analysis (TGA)

The thermal behavior of the drug and complexes was studied by heating the samples in pierced aluminum-crimped pans (pinhole) under nitrogen gas flow over the temperature range of 25–350 °C at a 10 °C min^{-1} heating rate. The samples containing MEG were performed only in the temperature range from 25 to 200 °C due to the premature thermal degradation of MEG. The DSC and TGA curves were obtained on a DSC TA 2920 and on a TGA TA 2920 equipment, respectively. Data were obtained and processed using the TA Instruments Universal Analysis 2000 software.

X-ray diffractometry (XRD)

The X-ray diffraction analyses were performed for pure substances, 1:1 FDS and 1:1 PM, using Rikugu®, model Dmax 2500PC X-ray diffractometer with a 2θ range between 4° and 50° using Cu Kα radiation ($\lambda = 1.5406$ Å) at scanning rate of 0.05°/min. The XRD patterns were recorded under ambient temperature conditions.

In vitro release studies

Release experiments of SMR and the complexes were carried out using a MicroettePlus® Vertical diffusion Franz cell apparatus with automatic sampling at 37 ± 2 °C and 300 rpm stirring rate (Hanson Research Corporation®). Cellulose acetate membrane with the pore size of 0.45 µm and exposed area of 1.77 cm^2 was used (Sigma Aldrich®, St. Louis, MO). Aqueous formulations (0.3 ml) with pure SMR, CD complexes or MEG binary system in the determined stoichiometric relation and in an oral dose quantity were loaded into the donor compartment. A 0.01 M phosphate buffer solution (PBS) of pH 7.4 was used as the diffusion medium in the donor and receptor cells. Samples (2.0 ml) were withdrawn from the receiver compartments at fixed intervals and replaced automatically with an equal volume of previously warmed PBS. SMR concentration was measured spectrophotometrically at 240 nm. The initial concentration of the drug or the complexes in PBS solution was held at 200 µg/ml.

Results and discussion

Phase solubility studies (PSS)

PSS of SMR in water, pH 2.0 and pH 8.0 solutions with βCD, MβCD, HPβCD and MEG are shown in Figure 2. In general, most of the isotherms can be classified as A_L-type diagrams according to Higuchi and Connors[38], as well as with the results previously reported by our research group for the SMR:βCD complex in water[37]. In these figures it is shown that the aqueous solubility of the drug increases linearly as a function of each ligand concentration with slope values less than unity, thus indicating the formation of 1:1 drug:CD complexes or drug:MEG binary systems, in accordance with the results of phase solubility studies published by several authors[24,39–42]. In exception, the isotherms of SMR with βCD in solutions of pH 8 resulted to be of A_N-type, which may be associated with the self-association of the CDs or with an alteration in the effective nature of the solvent in the presence of large concentrations of ligand, affecting the apparent degree of complexation, as explained in the review of Brewster and Loftsson[43]. On the other hand, the SMR:MEG system in solutions of pH 2.0 presented a decrease in SMR concentration as a function of MEG concentration, which was probably because both SMR and MEG present their amino groups protonated in this media ($pKa_{(SMR\ amine)} = 2.6$;[44] $pKa_{(MEG)} = 9.5$[45]) causing electrostatic repulsion that unfavors the formation of a binary system between them. Stability constants for the SMR:CDs complexes, calculated from the slope of the solubility diagrams, S_{max}, and solubility increments for all the systems are presented in Table 1. From these values, a different interaction between the drug and the CDs could be deduced. Because the weak sulfonamide acid group of SMR exists mainly in its unionized form at pH 2.0, the interactions with the CDs were produced more efficiently than at pH 8.0. Although drug complexation with cyclodextrins has been found to be better with the unionized drugs[46,47], the achieved total solubility significantly increased at pH 8.0 when the sulfonamide group of SMR was fully ionized. A similar behavior was observed with MEG. According to these results, it was possible to obtain a greater overall solubility by using a combined approach of pH adjustment and complexation with βCD, MβCD and HPβCD, or binary system formation with MEG. In contrast, the interaction of SMR with HPβCD showed a lower effectiveness when a buffer solution was used, which could be associated with the salt formation, because the effect of a third component probably depends on steric fit together with the drug in the cavity, as they act as space regulator. The solubility of the SMR:MEG system was higher than that which could be expected only by appropriate pH adjustment. It was found that the pH was increased to 9.5 at highest concentrations of MEG. Also, the percentages of the SMR moieties present at each pH were calculated using the Henderson–Hasselbalch equation, demonstrating that the SMR is about 100% in its anionic form at pH values reached by the addition of the quantities of MEG used in the studies (from pH 8.75 to 9.50) and even so the solubility continues growing. According to this, we can conclude that the enhancement in solubility might be due to a mechanism involving the formation of a strong ion pair between the drug and MEG.

Nuclear magnetic resonance (NMR) studies

^{1}H NMR spectra are one of the most direct evidence for the formation of the inclusion complexes[48]. The assignments and chemical shifts of the aliphatic MβCD, HPβCD and MEG protons and the aromatic SMR protons measured in D_2O before and after complexation are listed in Tables 2 and 3, respectively. For MβCD[49], HPβCD[50], MEG[51] and SMR[52], assignments of peaks to protons were performed following previous publications. The magnitude of the H_5 and H_3 shifts can be used as a measure of the complex stability as well as of the depth of inclusion[53]. Thus, in this study, the most significant downfield shifts were observed for the inner cavity CDs protons H_5 and H_3, and also for MβCD H_6 proton extending from the narrow rim of the βCD cavity. On the other hand, the relatively low shifts exhibited by protons at the outer surface of the CDs torus (H_1, H_2 and H_4) indicate lower or no interactions with the guest molecule. In addition, almost all SMR protons have been modified upon complexation, both upfield and downfield displacements were observed, probably due to van der Waals interactions[54] between SMR and the hydrophobic inner side of CDs. The most marked downfield displacements corresponded to H_A, H_C and H_E, which are located in meta positions from the sulfonamide group, and therefore, the lowest electron density gives them a greater affinity for the inner CD cavity. Also, these findings support the inclusion of the whole molecule into the CD cavity.

2D ROESY NMR is a technique frequently used to establish the connectivity between guest and host molecules in supramolecular complexation investigations[55,56]. In the 2D ROESY spectrum of MβCD and HPβCD with SMR (Figure 3), it is possible to observe intermolecular cross-peaks of H_B with H_5 and also with H_3 in SMR:MβCD. Furthermore, H_D presented interaction with H_5 and also with H_6 CDs protons in SMR:MβCD. These clearly indicate inclusion of SMR where the cavity protons (H_3, H_5) are affected by anisotropic shielding due to the

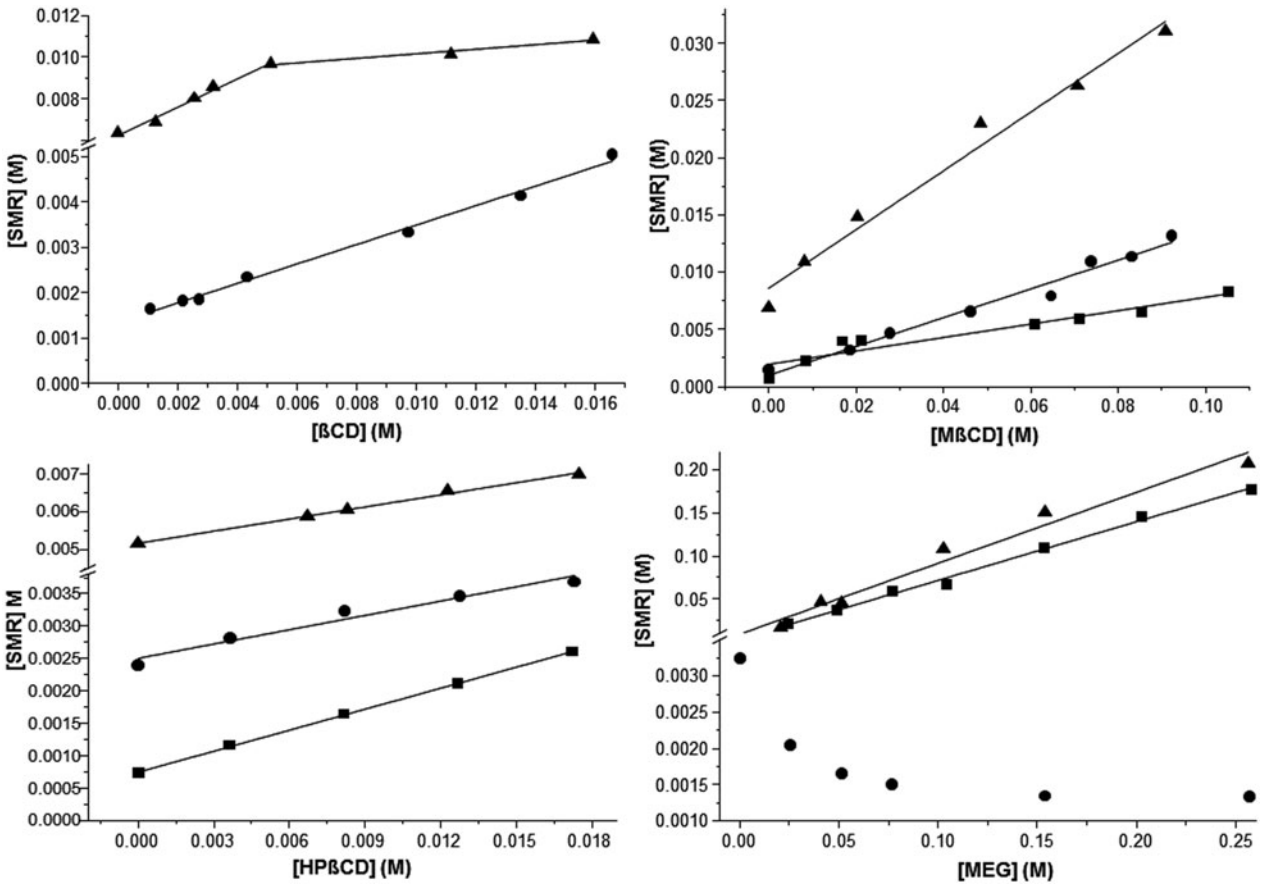

Figure 2. Phase solubility diagrams for sulfamerazine with βCD, MβCD, HPβCD and MEG at 25 °C in: water (■); pH 2.00 (●) and pH 8.00 (▲) solution.

Table 1. SMR solubilities, apparent 1:1 stability constants and solubility increments.

		βCD			MβCD			HPβCD			MEG	
Media	S_0 (mg/ml)	S_{max} (mg/ml)	K_c (M^{-1})	SI	S_{max} (mg/ml)	K_c (M^{-1})	SI	S_{max} (mg/ml)	K_c (M^{-1})	SI	S_{max} (mg/ml)	SI
Water	0.22 ± 0.04	0.83 ± 0.02 [23]	198 ± 22 [23]	3.20 [23]	2.2 ± 0.1	73 ± 21	10.0	0.69 ± 0.08	144 ± 26	3.14	46.8 ± 0.3	212.73
pH 2	0.32 ± 0.06	1.15 ± 0.08	207 ± 45	3.59	3.5 ± 0.1	118 ± 29	10.9	0.99 ± 0.01	65 ± 17	3.06	0.350 ± 0.001	1.09
pH 8	1.6 ± 0.2	3.768 ± 0.007	31 ± 8	2.4	8.1 ± 0.3	59 ± 13	1.1	1.9 ± 0.3	20 ± 4	1.2	54.8 ± 0.4	34.3

S_0: intrinsic solubility of the drug; S_{max}: Maximum solubility; K_C: stability constant of the complex; SI: solubility increment.

Table 2. Chemical shift of each ligand in the presence of SMR.

	δ MβCD	δ SMR:MβCD	Δδ	δ HPβCD	δ SMR:HPβCD	Δδ	δ MEG	δ SMR:MEG	Δδ
H_1	5.2507	5.2447	−0.0060	5.2517	5.2372	−0.0145	3.7241	3.7313	0.0072
H_{1a}	5.0638	5.0581	−0.0057	5.0978	5.0886	−0.0092	–	–	–
H_2		Overlapped with H_4		3.6489	3.6302	−0.0187	3.8673	4.0501	0.1828
H_{2a}	3.3841	3.3993	0.0152	–	–	–	–	–	–
H_3	4.0081	3.9952	−0.0129	3.9839	4.04575	0.06185	3.7916	3.7400	−0.0516
H_{3a}	3.9284	3.9541	0.0257	–	–	–	–	–	–
H_4		Overlapped with H_2		3.5214	3.5256	0.0042	3.6064	3.6220	0.0156*
H_5	3.6698	3.7985	0.1287	3.7454	3.8476	0.1022			
H_6	3.8624	3.8877	0.0253	3.8947	3.8932	−0.0015	2.6440	3.1618	0.5178
H_7	–	–	–	–	–	–	2.3251	2.7307	0.4056
OCH_3	3.5518	3.5788	0.0270	–	–	–			

a: metilated position
*undistinguishable

sulfonamide moiety and van der Waals interactions. This is in agreement with the data reported earlier for SMR, sulfadiazine and sulfamethazine with βCD by Zoppi et al.[37].

In SMR:MEG spectrum, downfield displacements of H_6 and H_7 of MEG and upfield displacements of all SMR protons were observed, which suggest that electrostatic interactions occurred, because the amine moiety of MEG may cause shielding in SMR protons in the proximity of the sulfonamide group. In addition, MEG H_2 downfield shift could indicate that van der Waals interactions also took place. The SMR:MEG 2D ROESY

Table 3. Chemical shifts of sulfamerazine in the presence of ligands.

	δ SMR	δ SMR:MβCD	Δδ	δ SMR:HPβCD	Δδ	δ SMR:MEG	Δδ
H_A	8.1764	8.3406	0.1624	8.2656	0.0892	8.0290	−0.1474
H_B	7.7369	7.7530	0.0161	7.7543	0.0174	7.6342	−0.1027
H_C	6.8670	6.9449	0.0779	6.8932	0.0262	6.7889	−0.0781
H_D	6.8091	6.6426	−0.1665	6.8034	−0.0057	6.6471	−0.1620
H_E	2.3901	2.4522	0.0621	2.4323	0.0422	2.2701	−0.1200

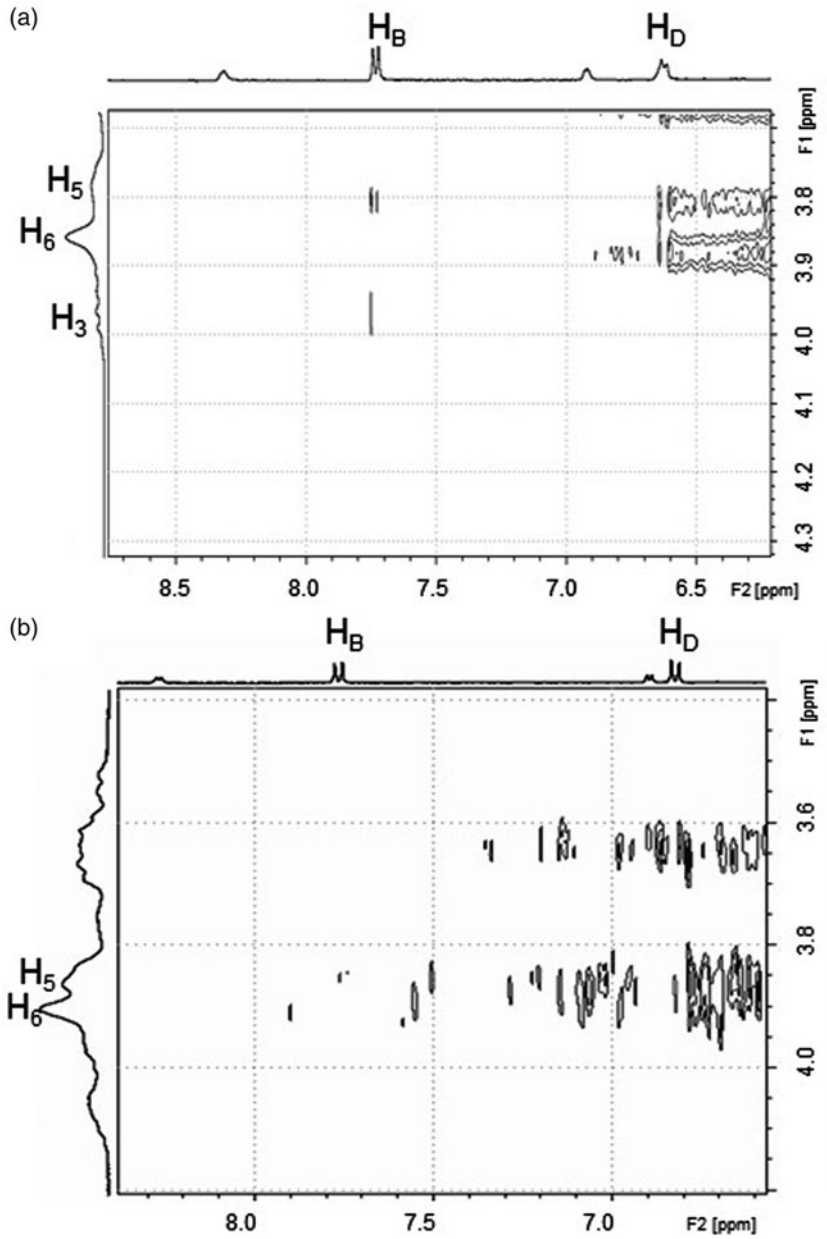

Figure 3. Partial contour plots of 2D ROESY spectrum of: (a) SMR:MβCD and (b) SMR:HPβCD complexes.

spectrum (Figure 4) confirm these interactions, because H_B and H_E presented cross-link peaks with H_2 and H_6, and H_E with H_7. We propose that a binary system between SMR and MEG was formed, where not only electrostatic forces were involved, but also van der Waals interactions were implicated.

Fourier-transform infrared spectroscopy (FT-IR)

FT-IR spectroscopy was used to assess the interaction between both CDs, MEG and SMZ in the solid state, because the changes in the shape, shift and intensity of the IR absorption peaks of the guest or host can provide enough information for the occurrence of the inclusion[57]. The FT-IR spectra of pure substances, FDS and PM of SMR with βCD, MβCD, HPβCD and MEG, are shown in Figure 5. Characteristic bands of SMR presented changes due to CD and MEG presence, as the aromatic ring vibration signals (1642 and 1630 cm^{-1}) which intensity relations were modified with βCD and MβCD FDS or disappeared with HPβCD. Also, changes in the intensities of the peaks at 1596 and 1555 cm^{-1} were exhibited. Furthermore, the relative intensities of symmetric and asymmetric SO_2 stretching peaks (1327 and 1303 cm^{-1}) were modified with MEG and HPβCD FDS, and the S=O stretching

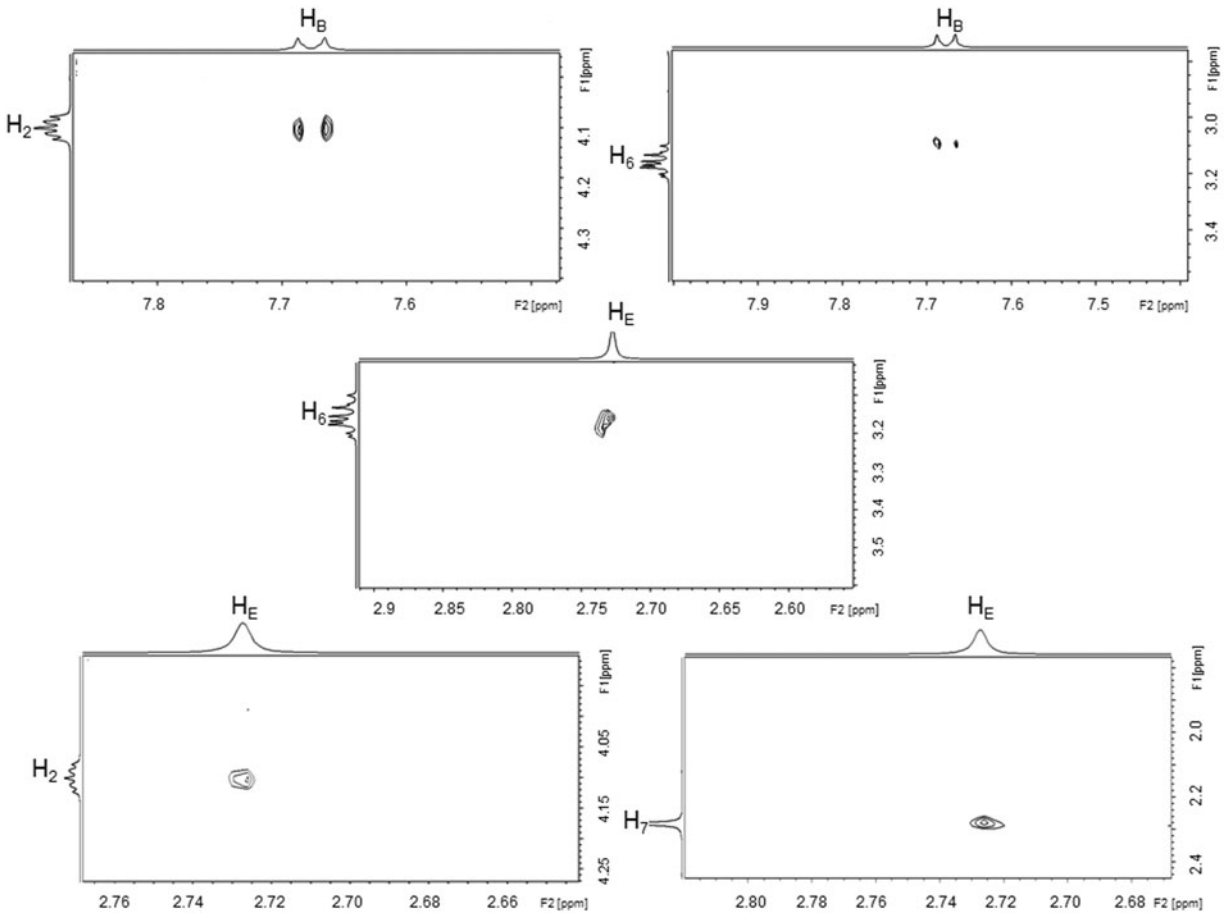

Figure 4. Partial contour plots of 2D ROESY spectrum of SMR:MEG binary system.

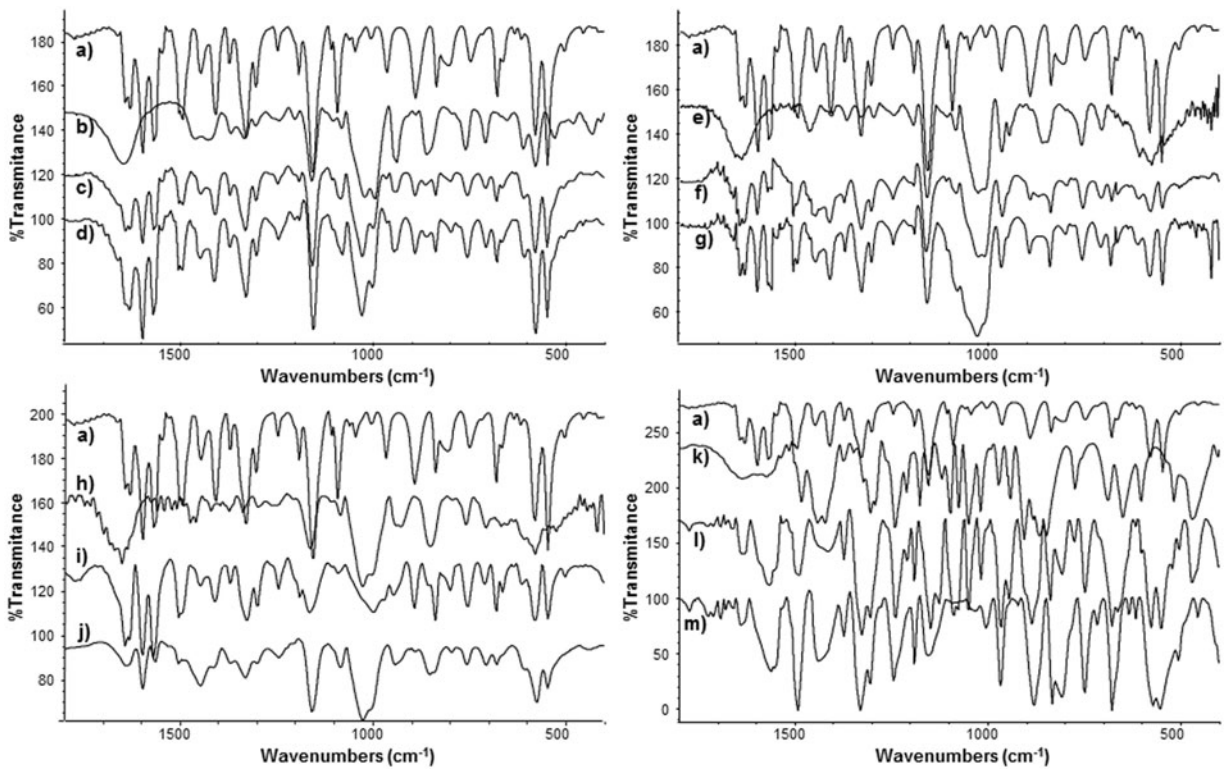

Figure 5. FT-IR spectra of: (a) pure SMR; (b) pure βCD; (c) SMR:βCD 1:1 PM; (d) SMR:βCD 1:1 FDS; (e) pure MβCD; (f) SMR:MβCD 1:1 PM; (g) SMR:MβCD 1:1 FDS; (h) pure HPβCD; (i) SMR:HPβCD 1:1 PM; (j) SMR:HPβCD 1:1 FDS; (k) pure MEG; (l) SMR:MEG 1:1 PM; (m) SMR:MEG 1:1 FDS.

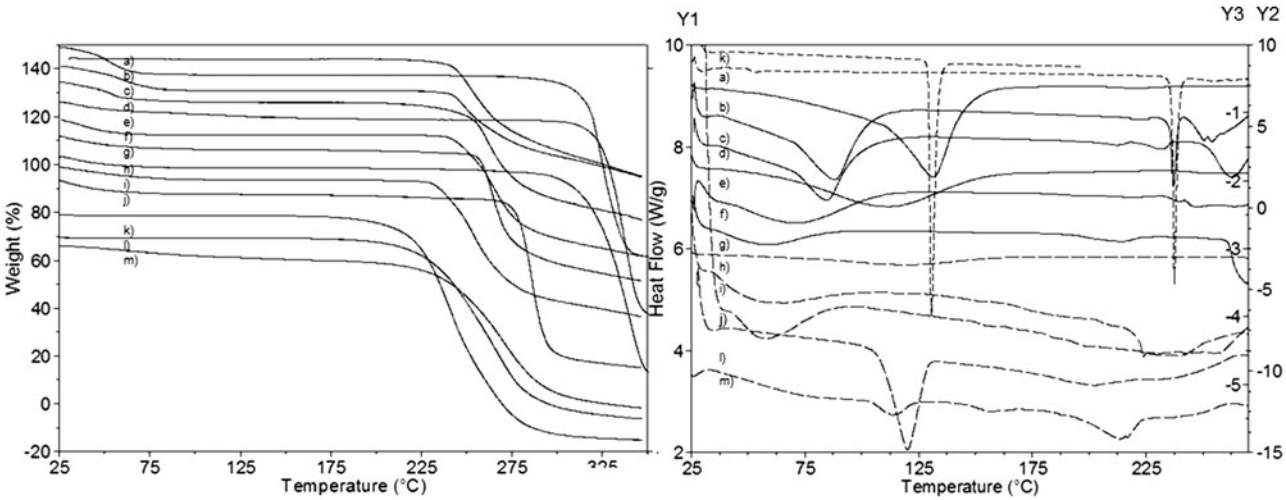

Figure 6. DSC and TG curves of: (a) pure SMR; (b) pure βCD; (c) SMR:βCD 1:1 PM; (d) SMR:βCD 1:1 FDS; (e) pure MβCD; (f) SMR:MβCD 1:1 PM; (g) SMR:MβCD 1:1 FDS; (h) pure HPβCD; (i) SMR:HPβCD 1:1 PM; (j) SMR:HPβCD 1:1 FDS; (k) pure MEG; (l) SMR:MEG 1:1 PM; (m) SMR:MEG 1:1 FDS. Scales: Y1, short dashed line; Y2, solid line; Y3, dashed line.

band (1092 cm^{-1}) was shifted to lower frequencies in SMR:βCD PM and FDS (1087 and 1090 cm^{-1}, respectively). In addition, many other signals located in the fingerprint region of SMR were observed to have inverted their relative intensities or were shifted to lower frequencies in FDS compared with the PM of SMR with MβCD, HPβCD and MEG systems. On the other hand, a MEG band corresponding to the O–H bond vibration on plane was shifted to a higher frequency (1239 to 1245 cm^{-1}) due to the presence of SMR in the FDS. The differences between the PM and the FDS profiles may suggest the formation of true inclusion complexes of SMR with the CDs and binary systems of SMR with MEG when they are prepared by means of lyophilization.

Differential scanning calorimetry (DSC) and thermogravimetric analysis (TGA)

DSC and TGA are frequently the pharmaceutical thermal analysis techniques of choice for studying complexation, due to their ability to provide detailed information about both the physical and energetic properties of substances[58]. Figure 6 illustrates the TGA and DSC profiles of SMR, CDs, MEG, the PM and corresponding FDS. The SMR thermal curve was typical of a crystalline substance and was characterized by a sharp endothermic peak (temperature at 237.51 °C), assigned to its melting point, and decomposing above 270 °C. As can be observed by a comparison of the TGA and DSC curves, CDs lose water at temperatures in the range from 25 to 150 °C and decompose above 250 °C, as evidenced by the mass loss in the TGA curves. The PMs of CDs and SMR not only presented the endothermic peaks due to melting of the drug, followed by decomposition, represented by a continuous mass loss in the TGA curves, but also these curves presented shifts on temperature and changes in mass loss of the dehydration event. Besides, in SMR:HPβCD PM, the SMR melting peak slightly shifted to lower temperatures. These events could be explained by the weak molecular interactions between the SMR and CDs at high temperatures, but these were not evidences of the formation of true inclusion compounds. In addition, the melting peak of free SMR is absent in the DSC curves of the lyophilized samples, and also these curves presented shifts on the corresponding CD dehydration temperature and changes in mass loss. The SMR:βCD and SMR:MβCD FDS curves also present thermal events at 211.92 °C/232.35 °C and 212.73 °C, respectively, absent in the curve of free SMR. We suggest that these events may be related to the melting of non-included drug or to the beginning of decomposition, because the first peak of each one coincides with the beginning of mass loss in the TGA curve. The differences between the PM and the FDS profiles may suggest the formation of true inclusion complexes of SMR with the CDs when they are prepared by means of lyophilization. On the other hand, as like SMR, MEG DSC curve presents a sharp endothermic peak with no loss of weight, corresponding to its melting point, and decomposing above 200 °C. In SMR:MEG PM curve, the endothermic peak corresponding to MEG melting point broadened and shifted to lower temperatures, which may indicate the interaction between the components. Besides, this signal disappeared in the FDS, and also the decomposition occurred at higher temperature and with a lower mass loss, probably demonstrating the formation of a new entity with higher thermal stability. Also, there are three events presented on the FDS DSC curve at 113.55 °C, 155.44 °C and 213.37 °C, which may correspond to the melting of the remaining free MEG and drug, and to the beginning of decomposition, respectively. The relative crystallinity of MEG (MEG_{RDC}) in PM and FDS was estimated by the ratio between the melting enthalpy of MEG calculated in the sample (ΔH_{sample}) and that of the pure MEG (ΔH_{MEG}), according to the following equation[59]:

$$MEG_{RDC} = \Delta H_{sample}/\Delta H_{MEG}$$

Where ΔH_{sample} is the melting enthalpy of MEG calculated in the physical mixture or complex, and ΔH_{MEG} is the melting enthalpy of the pure MEG. The values reported in Table 4 show that the FDS resulted to have less crystallinity than the PM, which may indicate that the formation of a binary system between SMR and MEG occurred.

Table 4. MEG_{RDC} for the physical mixture and freeze-dried system of SMR with MEG.

ΔH_{MEG} (J/g)	$\Delta H_{SMR:MEG\ PM}$ (J/g)	$\Delta H_{SMR:MEG\ FDS}$ (J/g)	MEG_{RDC} in PM	MEG_{RDC} in LIO
264.7	98.78	14.05	0.37	0.05

X-ray diffractometry (XRD)

Powder XRD is a suitable method for determining the molecular state of a complex[60]. Figure 7 shows the X-ray diffraction patterns of SMR and the corresponding PM of the lyophilized components

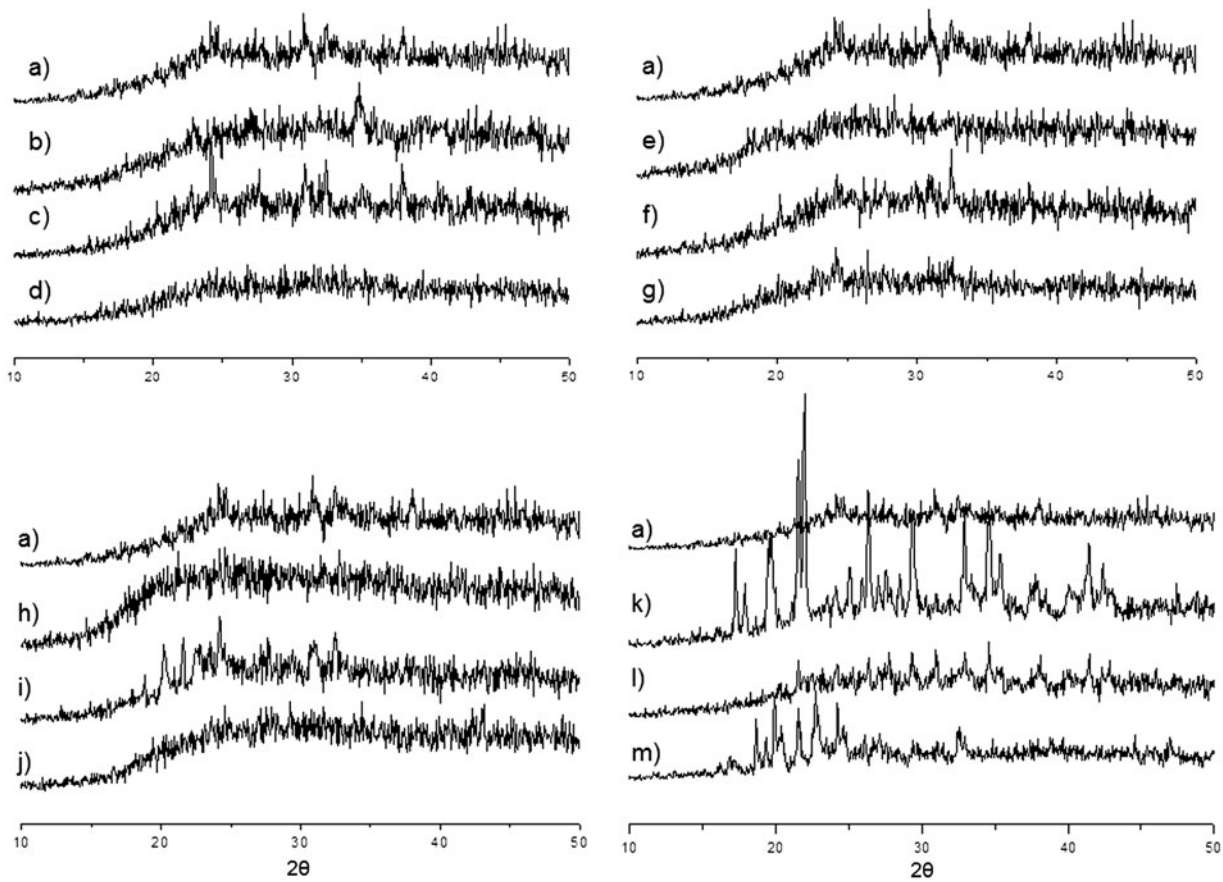

Figure 7. DRX patterns of: (a) pure SMR; (b) pure βCD; (c) SMR:βCD 1:1 PM; (d) SMR:βCD 1:1 FDS; (e) pure MβCD; (f) SMR:MβCD 1:1 PM; (g) SMR:MβCD 1:1 FDS; (h) pure HPβCD; (i) SMR:HPβCD 1:1 PM; (j) SMR:HPβCD 1:1 FDS; (k) pure MEG; (l) SMR:MEG 1:1 PM; (m) SMR:MEG 1:1 FDS.

Figure 8. Permeation profiles of: SMR (▼); SMR:βCD 1:1 complex (■); SMR:MβCD 1:1 complex (▲); SMR:HPβCD 1:1 complex (►); SMR:MEG 1:1 binary system (●); (each value represents the mean ± S.D. of $n \geq 3$).

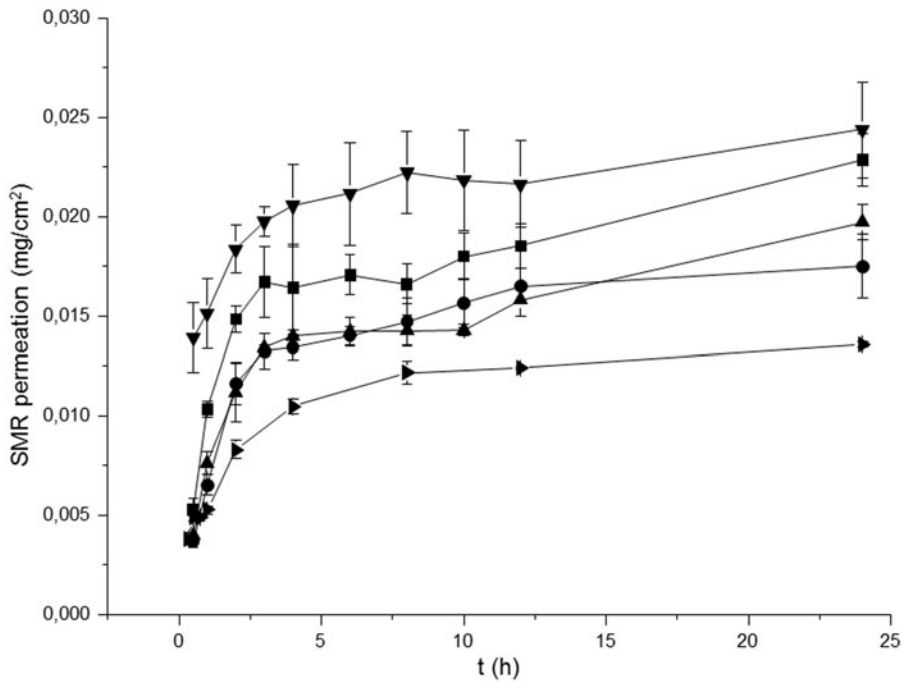

or FDS with CDs and MEG. In the X-ray diffraction pattern of SMR powder, the sharp peaks present at $2\theta = 24.2°$, 24.7°, 27.4°, 28.9°, 29.9°, 30.8°, 32.4°, 36.7°, 38.0°, 44.9° and 45.5° suggest that the drug is present as a crystalline material, as well as MEG whose crystalline patterns presented sharp peaks at $2\theta = 17.1°$, 18.1°, 19.7°, 21.6°, 21.9°, 26.2°, 29.5°, 32.9°, 34.5°, 35.3°, 38.0°, 41.5° and 42.4°. The βCD also exhibited a typical crystalline diffraction pattern (at $2\theta = 22.9°$, 27.1°, 34.9°), but MβCD and HPβCD presented amorphous character. For evaluating the effect of the freeze-dried procedure on the crystallinity of the

components, the lyophilized pure substances diffraction patterns of SMR, βCD and MEG are presented. The XRD patterns of the PMs confirmed the presence of each species as isolated solid, because the diffraction patterns showed SMR, βCD or MEG peaks or the amorphous halo of MβCD or HPβCD, respectively. A total drug amorphization was instead induced by freeze-drying where X-ray diffraction patterns of SMR:CDs systems were characterized only by large diffraction bands in which it is no longer possible to distinguish the characteristic peaks of the drug. These results suggest that SMR is no longer present as a crystalline material and its CD solid complexes exist in the amorphous state. On the other hand, some crystalline diffraction peaks are still detectable in SMR:MEG FDS attributable to MEG crystals, which could correspond to the presence of an excess of isolated MEG. There was no coincidence with SMR XRD pattern, and peaks at different diffraction angle appeared, suggesting that a new entity with distinct crystalline order than the isolated components was formed.

In vitro release studies

The ability of the CDs and MEG to host SMR and to sustain its release was tested.

As a general trend the complexes showed sustained release of the drug (Figure 8). Also, it was observed that all formulations containing CD or MEG exhibited lower permeation compared to SMR alone. This finding suggests that SMR was indeed taken up by the CDs and MEG and, then, slowly released.

The CDs and MEG led to smaller release in comparison with the SMR alone. That is, the CDs and MEG enabled sustained drug delivery.

Conclusions

Inclusion binary complexes with CDs and MEG binary systems formation was demonstrated by NMR, IR, DSC/TGA and XRD. CD complexes showed significant improvement in solubilization compared with the free drug. MEG was responsible for solubility improvement via multiple factors rather than just providing a favorable pH, and also the higher solubility enhancement was achieved with the combined approach of binary systems formation with MEG and pH adjustment. Permeation studies demonstrated that the complexation with βCD, MβCD, HPβCD and MEG resulted in a decrease in release rate of the drug through cellulose acetate membrane, enabling sustained drug delivery systems. These findings have relevant applications in the preparation of an oral dosage form containing the drug.

Acknowledgements

Financial support from ''Fondo para la Investigación Científica y Tecnológica'' (FONCYT) Préstamo BID 1728/OC-AR PICT 1376, ''Consejo Nacional de Investigaciones Científicas y Técnicas'' (CONICET) and ''Secretaría de Ciencia y Técnica de la Universidad Nacional de Córdoba'' (SECyT-UNC) are greatly acknowledged. Dr Gloria M. Bonetto's assistance and her helpful discussion in NMR measurements are highly appreciated. We also thank Ferromet S.A. (Roquette's agent in Argentina) for their donation of cyclodextrins. We also thank Dr. Paul Hobson, native speaker, for revision of the manuscript.

Declaration of interest

The authors report no declarations of interest.

References

1. European Pharmacopoeia. 7th ed.; 2010.
2. Kasim N, Whitehouse M, Ramachandran C, et al. Molecular properties of WHO essential drugs and provisional biopharmaceutical classification. Mol Pharm 2004;1:85–96.
3. Fuchs SM, Elsner P. Sulfonamides in dermatology. Dis Mon 2004; 50:280–90.
4. Vassiliou AA, Papadimitriou SA, Bikiaris DN, et al. Facile synthesis of polyester-PEG triblock copolymers and preparation of amphiphilic nanoparticles as drug carriers. J Control Release 2010;148:388–95.
5. Arakawa T, Kita Y, Koyama AH. Solubility enhancement of gluten and organic compounds by arginine. Int J Pharm 2008;355:220–3.
6. Bimbo LM, Mäkilä E, Laaksonen T, et al. Drug permeation across intestinal epithelial cells using porous silicon nanoparticles. Biomaterials 2011;32:2625–33.
7. Breda SA, Jimenez-Kairuz AF, Manzo RH, Olivera ME. Solubility behavior and biopharmaceutical classification of novel high-solubility ciprofloxacin and norfloxacin pharmaceutical derivatives. Int J Pharm 2009;371:106–13.
8. Li G, Fan Y, Li X, et al. *In vitro* and *in vivo* evaluation of a simple microemulsion formulation for propofol. Int J Pharm 2012;425: 53–61.
9. Maestrelli F, Cirri M, Mennini N, et al. Improvement of oxaprozin solubility and permeability by the combined use of cyclodextrin, chitosan, and bile components. Eu J Pharm Bio 2011;78:385–93.
10. de Araújo MVG, Vieira EKB, Silva Lázaro G, et al. Sulfadiazine/hydroxypropyl-[beta]-cyclodextrin host-guest system: characterization, phase-solubility and molecular modeling. Bioorg Med Chem 2008;16:5788–94.
11. Yang B, Lin J, Chen Y, Liu Y. Artemether/hydroxypropyl-[beta]-cyclodextrin host-guest system: characterization, phase-solubility and inclusion mode. Bioorg Med Chem 2009;17:6311–17.
12. Iohara D, Hirayama F, Ishiguro T, et al. Preparation of amorphous indomethacin from aqueous 2,6-di-O-methyl-[beta]-cyclodextrin solution. Int J Pharm 2008;354:70–6.
13. Li N, Wei X, Mei Z, et al. Synthesis and characterization of a novel polyamidoamine–cyclodextrin crosslinked copolymer. Carbohydr Res 2011;346:1721–7.
14. Doyagüez EG, Fernández-Mayoralas A. Proline–cyclodextrin conjugates: synthesis and evaluation as catalysts for aldol reaction in water. Tetrahedron 2012;68:7345–54.
15. Zhang G, Liang F, Song X, et al. New amphiphilic biodegradable β-cyclodextrin/poly(l-leucine) copolymers: synthesis, characterization, and micellization. Carbohyd Polym 2010;80:885–90.
16. Guan Z, Wang Y, Chen Y, et al. Novel approach for synthesis of 2:1 permethylated β-cyclodextrin–C60 conjugate. Tetrahedron 2009;65: 1125–9.
17. Wang R-Q, Ong T-T, Ng S-C. Synthesis of cationic β-cyclodextrin derivatives and their applications as chiral stationary phases for high-performance liquid chromatography and supercritical fluid chromatography. J Chromatogr A 2008;1203:185–92.
18. dos Santos J-FR, Couceiro R, Concheiro A, et al. Poly(hydroxyethyl methacrylate-co-methacrylated-β-cyclodextrin) hydrogels: synthesis, cytocompatibility, mechanical properties and drug loading/release properties. Acta Biomater 2008;4:745–55.
19. Kutyła MJ, Lambert LK, Davies NM, et al. Cyclodextrin-crosslinked poly(acrylic acid): synthesis, physicochemical characterization and controlled release of diflunisal and fluconazole from hydrogels. Int J Pharm 2013;444:175–84.
20. Kumar N, Shishu GB, Bansal G, et al. Preparation and cyclodextrin assisted dissolution rate enhancement of itraconazolium dinitrate salt. Drug Dev Ind Pharm 2013;39:342–51.
21. Granero GE, Maitre MM, Garnero C, Longhi MR. Synthesis, characterization and in vitro release studies of a new acetazolamide-HP-[beta]-CD-TEA inclusion complex. Eur J Med Chem 2008;43: 464–70.
22. Garnero C, Longhi M. Study of ascorbic acid interaction with hydroxypropyl-[beta]-cyclodextrin and triethanolamine, separately and in combination. J Pharmaceut Biomed 2007;45:536–45.
23. Zoppi A, Garnero C, Linck YG, et al. Enalapril:[beta]-CD complex: stability enhancement in solid state. Carbohyd Polym 2011;86: 716–21.
24. Özdemir N, Erkin J. Enhancement of dissolution rate and bioavailability of sulfamethoxazole by complexation with β-cyclodextrin. Drug Dev Ind Pharm 2012;38:331–40.
25. Lu Y, Zhang T, Tao J, et al. Preparation, characterization, and pharmacokinetics of the inclusion complex of genipin-β-cyclodextrin. Drug Dev Ind Pharm 2009;35:1452–59.

26. Granero GE, Garnero C, Longhi M. The effect of pH and triethanolamine on sulfisoxazole complexation with hydroxypropyl-[beta]-cyclodextrin. Eur J Pharm Sci 2003;20:285–93.
27. Gundogdu E, Koksal C, Karasulu E. Comparison of cefpodoxime proxetil release and antimicrobial activity from tablet formulations: complexation with hydroxypropyl-β-cyclodextrin in the presence of water soluble polymer. Drug Dev Ind Pharm 2012;38:689–96.
28. Stefani Borghetti G, Pinheiro Pinto A, Silva Lula I, et al. Daidzein/cyclodextrin/hydrophilic polymer ternary systems. Drug Dev Ind Pharm 2011;37:886–93.
29. Mou D, Chen H, Wan J, et al. Potent dried drug nanosuspensions for oral bioavailability enhancement of poorly soluble drugs with pH-dependent solubility. Int J Pharm 2011;413:237–44.
30. Morand K, Bartoletti AC, Bochot A, et al. Liposomal amphotericin B eye drops to treat fungal keratitis: physico-chemical and formulation stability. Int J Pharm 2007;344:150–3.
31. Serajuddin ATM. Salt formation to improve drug solubility. Adv Drug Deliv Rev 2007;59:603–16.
32. Tarsa PB, Towler CS, Woollam G, Berghausen J. The influence of aqueous content in small scale salt screening – improving hit rate for weakly basic, low solubility drugs. Eur J Pharm Sci 2010;41:23–30.
33. Gupta P, Bansal AK. Ternary amorphous composites of celecoxib, poly(vinyl pyrrolidone) and meglumine with enhanced solubility. Die Pharmazie 2005;60:830–6.
34. Frézard F, Martins PS, Bahia APCO, et al. Enhanced oral delivery of antimony from meglumine antimoniate/β-cyclodextrin nanoassemblies. Int J Pharm 2008;347:102–8.
35. Gupta P, Bansal AK. Modeling of drug release from celecoxib-PVP-meglumine amorphous system. PDA J Pharm Sci Technol 2005;59:346–54.
36. Gupta P, Bansal AK. Molecular interactions in celecoxib-PVP-meglumine amorphous system. J Pharm Pharmacol 2005;57:303–10.
37. Zoppi A, Quevedo MA, Delrivo A, Longhi MR. Complexation of sulfonamides with β-cyclodextrin studied by experimental and theoretical methods. J Pharm Sci 2009;99:3166–76.
38. Higuchi T, Connors K. Phase solubility thechniques. In: Reilly C, ed. Advances in analytical chemistry and instrumentation. New York: Wiley/Interscience; 1965:117–212.
39. Ge X, Huang Z, Tian S, et al. Complexation of carbendazim with hydroxypropyl–cyclodextrin to improve solubility and fungicidal activity. Carb Pol 2012;89:208–12.
40. Rosa dos Santos J, Couceiro R, Concheiro A, et al. Poly(hydroxyethyl methacrylate-co-methacrylated-b-cyclodextrin) hydrogels: synthesis, cytocompatibility, mechanical properties and drug loading/release properties. Acta Biomat 2008;4:745–55.
41. Maestrelli F, Cirri M, Mennini N, et al. Improvement of oxaprozin solubility and permeability by the combined use of cyclodextrin, chitosan, and bile components. Eur J Pharm Biopharm 2011;78:385–93.
42. Shia JH, Zhoua Yf. Inclusion interaction of chloramphenicol and heptakis (2,6-di-O-methyl)-β-cyclodextrin: phase solubility and spectroscopic methods. Spect Acta Part A 2011;83:570–4.
43. Brewster ME, Loftsson T. Cyclodextrins as pharmaceutical solubilizers. Adv Drug Dev Rev 2007;59:645–66.
44. Qiang Z, Adams C. Potentiometric determination of acid dissociation constants (pKa) for human and veterinary antibiotics. Water research 2004;38:2874–90.
45. Basavaraj S, Sihorkar V, Shantha Kumar TR, et al. Bioavailability enhancement of poorly water soluble and weakly acidic new chemical entity with 2-hydroxy propyl-β-cyclodextrin: selection of meglumine, a polyhydroxy base, as a novel ternary component. Pharm Dev Technol 2006;11:443–51.
46. Linares M, de Bertorello MM, Longhi M. Solubilization of naphthoquinones by complexation with hydroxypropyl-[beta]-cyclodextrin. Int J Pharm 1997;159:13–18.
47. Al Omari MM, Daraghmeh NH, El-Barghouthi MI, et al. Novel inclusion complex of ibuprofen tromethamine with cyclodextrins: physico-chemical characterization. J Pharmaceut Biomed 2009;50:449–58.
48. Schneider HJ, Hacket F, Rüdiger V. NMR studies of cyclodextrins and cyclodextrin complexes. Chem Rev 1998;98:1755–85.
49. Delrivo A, Zoppi A, Longhi MR. Interaction of sulfadiazine with cyclodextrins in aqueous solution and solid state. Carb Pol 2012;87:1980–88.
50. Loukas Y, Vraka V, Gregoriadis G. Use of a nonlinear least-squares model for the kinetic determination of the stability constant of cydodextrin inclusion complexes. Int J Pharm 1996;144:225–31.
51. Roberts WL, McMurray WJ, Rainey PM. Characterization of the antimonial antileishmanial agent meglumine antimonate (glucantime). Antimicrob Agents Chemother 1998;42:1076–82.
52. Turczan J, Medwick T. Identification of sulfonamides by NMR spectroscopy. J Pharm Sci 1972;61:434–43.
53. Rekharsky M, Goldberg R, Schwarz F, et al. Thermodynamic and nuclear magnetic resonance study of the interactions of α- and β-cyclodextrin with model substances: phenethylamine, ephedrines, and related substances. J Am Chem Soc 1995;117:8830–40.
54. Anguiano-Igea S, Otero-Espinar FJ, Vila-Jato JL, Blanco-Méndez J. Interaction of clofibrate with cyclodextrin in solution: phase solubility,1H NMR and molecular modelling studies. Eur J Pharm Sci 1997;5:215–21.
55. Linde GA, Laverde Junior A, Vaz de Faria E, et al. The use of 2D NMR to study β-cyclodextrin complexation and debittering of amino acids and peptides. Food Res Int 2010;43:187–92.
56. Jullian C, Cifuentes C, Alfaro M, et al. Spectroscopic characterization of the inclusion complexes of luteolin with native and derivatized β-cyclodextrin. Bioorg Med Chem 2010;18:5025–31.
57. Szente L, Osa T, eds., Comprehensive supramolecular chemistry. Vol. 3. Oxford: Pergamon Press; 1996:253–78.
58. Clas SD, Dalton CR, Hancock BC. Differential scanning calorimetry: applications in drug development. Pharm Sci Tech Today 1999;2:311–20.
59. Li N, Xu L. Thermal analysis of [beta]-cyclodextrin/Berberine chloride inclusion compounds. Thermochim Acta 2010;499:166–70.
60. Aignera Z, Berkesib O, Farkasa G, Szabó-Révésza P. DSC, X-ray and FTIR studies of a gemfibrozil/dimethyl–cyclodextrin inclusion complex produced by co-grinding. J Pharm Biomed 2012;57:62–7.